


## Article

# Analysis of Spatiotemporal Evolution and Influencing Factors of Vegetation Net Primary Productivity in the Yellow River Basin from 2000 to 2022

Kunjun Tian <sup>1</sup>, Xing Liu <sup>1,\*</sup>, Bingbing Zhang <sup>2</sup>, Zhengtao Wang <sup>3</sup> , Gong Xu <sup>1</sup>, Kai Chang <sup>1</sup>, Pengfei Xu <sup>1</sup> and Baomin Han <sup>1</sup>

<sup>1</sup> School of Civil Engineering and Geomatics, Shandong University of Technology, Zibo 255049, China; kjtian@sdut.edu.cn (K.T.); xugong1983@163.com (G.X.); changkainenu@163.com (K.C.); xupengfei@sdut.edu.cn (P.X.); hanbm@sdut.edu.cn (B.H.)

<sup>2</sup> School of Geographic Sciences, Xinyang Normal University, Xinyang 464000, China; bbzhang@xynu.edu.cn

<sup>3</sup> School of Geodesy and Geomatics, Wuhan University, Wuhan 430079, China; ztwang@whu.edu.cn

\* Correspondence: 22507020022@stumail.sdut.edu.cn

**Abstract:** The Yellow River Basin (YRB) plays a very important role in China's economic and social development and ecological security, so studying the spatiotemporal variation characteristics of net primary productivity (NPP) and its influencing factors is of great significance for protecting the stable development of its ecological environment. This article takes the YRB as the research area, based on Moderate Resolution Imaging Spectroradiometer (MODIS) data, climate data, terrain data, land data, social data, and the gravity recovery and climate experiment (GRACE) data. The spatiotemporal evolution characteristics of vegetation NPP in the YRB from 2000 to 2022 were explored using methods such as trend analysis, correlation analysis, and geographic detectors, and the correlation characteristics of NPP with meteorological factors, social factors, and total water storage (TWS) were evaluated. The results indicate that the NPP of vegetation in the YRB showed an increasing trend ( $4.989 \text{ gC}\cdot\text{m}^{-2}\cdot\text{a}^{-1}$ ) from 2000 to 2022, with the most significant changes occurring in the middle reaches of the YRB. The correlation coefficient indicates that temperature and accumulated temperature have a significant positive impact on the change of NPP, while TWS has a significant negative impact. In the study of the factors affecting vegetation NPP in the YRB, the most influential factors are soil type (0.48), precipitation (0.46), and temperature (0.32). The strong correlation between TWS and vegetation NPP in the YRB is about 39%, with a contribution rate of about 0.12, which is a factor that cannot be ignored in studying vegetation NPP changes in the YRB.

**Keywords:** vegetation NPP; Yellow River Basin; total water storage; climate change; spatiotemporal evolution



**Citation:** Tian, K.; Liu, X.; Zhang, B.; Wang, Z.; Xu, G.; Chang, K.; Xu, P.; Han, B. Analysis of Spatiotemporal Evolution and Influencing Factors of Vegetation Net Primary Productivity in the Yellow River Basin from 2000 to 2022. *Sustainability* **2024**, *16*, 381. <https://doi.org/10.3390/su16010381>

Academic Editor: Tommaso Caloiero

Received: 7 December 2023

Revised: 25 December 2023

Accepted: 27 December 2023

Published: 31 December 2023



**Copyright:** © 2023 by the authors. Licensee MDPI, Basel, Switzerland. This article is an open access article distributed under the terms and conditions of the Creative Commons Attribution (CC BY) license (<https://creativecommons.org/licenses/by/4.0/>).

## 1. Introduction

Gross primary productivity (GPP) is known as the quantity of organic matter accumulated by green plants per unit area over a specific period. NPP is the remainder obtained by subtracting Autotrophic Respiration (RA) from GPP [1]. NPP serves as a vital parameter for assessing changes in terrestrial ecosystems and evaluating their sustainability [2–4]. It is one of the key indicators of the material foundation for ecosystem development [5,6] and plays a significant role in ecosystem assessment processes [7–10]. Furthermore, it is influenced by climate change [11–14].

The 75th United Nations General Assembly in 2020 pointed out the importance of achieving carbon neutrality and reducing carbon emissions. Vegetation NPP is essential for estimating carbon sources and sinks in terrestrial ecosystems and describing the processes of carbon cycling and energy flow [15,16]. Over the past century, experts and scholars have continuously conducted research on NPP estimation methods, spatiotemporal distribution,

and influencing factors from various perspectives [17–19]. Significant progress has been made in this field. Today, the relationship between terrestrial ecosystems and climate change remains a focus of global change research [20–22]. Largely, work has been performed to improve NPP models. Lieth [23,24] developed the Miami model, while Runing and others introduced the BIOME-BGC model. Potter and his team [25] conducted studies to enhance the CASA model. In 1995, Field and others [26] analyzed this model and discussed its limitations and shortcomings. They made optimizations to address these limitations. Chinese scholars have also conducted relevant research and proposed models such as the Zhou Guangsheng-Zhang Xinshi and Zhu Zihui models [27,28]. In the progress of spatiotemporal evolution research, domestic and international scholars have conducted extensive research on vegetation conditions using vegetation NPP data based on different spatiotemporal scales; for example, in regions such as the western United States [29], southeastern Tunisia [30], Japan [31], Greenland [32], the entire territory of China [33], the eastern part of East China [34], the northwestern region [35], and the Yangtze River Basin [36]. However, due to the influence of variations in vegetation's physiological characteristics, NPP exhibits significant spatiotemporal heterogeneity at different regional scales [37], making it challenging to determine the driving mechanisms behind spatiotemporal changes in NPP at the regional scale [38–40].

The ecological environment of the YRB deeply affects the economic and social development of northern China and even the whole country. However, the ecological climate of the YRB is complex, and many environmental problems have emerged in recent years. Therefore, a comprehensive understanding of the spatiotemporal variation characteristics of vegetation NPP in the YRB and an in-depth exploration of its influencing factors are of great significance for China's sustainable development.

In recent years, many scholars have studied the changes in the NPP in the YRB. Zhang et al. [41] used MODIS NPP data products, along with a quantitative net ecosystem productivity (NEP) estimation model, and systematically analyzed the ecological changes in this region. Jiang et al. [42], using remote sensing data, MODIS NPP, and meteorological data, studied the spatiotemporal transformation of NPP and Precipitation Use Efficiency (PUE). Yang and Li [43] used fossil fuel carbon emission grid data and land use data and studied the spatiotemporal heterogeneity and driving mechanisms of the Yellow River Delta. Zhang and Liu [44] conducted studies on the spatiotemporal variation characteristics of five urban agglomerations using spatial expansion measurements, centroid shifts, urban primacy, and gravity models. Liu et al. [45] constructed ecological restoration evaluation indicators, systematically analyzed the impact of climate and human activities on the environment, and comprehensively evaluated the ecological restoration status and potential of the upper reaches of the Yellow River. Tian et al. [46] used various analysis methods to study the spatiotemporal variation characteristics of NPP in the YRB over the past 40 years and quantified the impact of meteorological factors on it. Zhang et al. [47] quantitatively assessed the relationship between changes in NPP and human activities and climate in the high-altitude grasslands from 2000 to 2020. Xue et al. [48] analyzed the spatiotemporal variation characteristics of NPP in the upstream region using the random forest method. Wei et al. [49] studied the spatiotemporal variation of NPP based on adjusted ecological parameter factors. Song et al. [50] assessed NPP changes in the Sanjiangyuan area from 2000 to 2019 using the Carnegie–Ames–Stanford Approach (CASA) model. Xuan and Rao [51] studied the spatiotemporal variation characteristics and influencing factors of NPP in the midstream region from 2000 to 2020. Chen et al. [52] studied variations in NPP in parts of the Loess Plateau. Zhu et al. [53] combined RS and GIS methods to analyze the ecological changes in the YRB. Hong et al. [54] studied the temporal and spatial variation of vegetation NPP and its driving factors in Ningxia.

Regarding the driving mechanisms of NPP in the YRB, numerous scholars have separately studied the impacts of climate change [45–47,50,55–57], human activities [45,50,56,58–60], vegetation types [48], and precipitation [42] on NPP. Zhang et al. [61] investigated the response of NPP to soil pH and evaluated their impact on grassland ecosystems. Water plays

an irreplaceable role in plant growth, and some scholars have researched the relationship between water availability and changes in NPP in the YRB. Zhou et al. [62] used different models to estimate NPP, soil retention, and water resources and analyzed the synergies among ecosystems. Shao et al. [63] simulated NPP, water yield, grain production, soil retention, and habitat quality. They assessed the spatial evolution of ecosystems and their driving factors at the grid scale. But, in these research studies, water yield is the difference between precipitation and evapotranspiration, which may introduce some errors in water quantity estimation. The GRACE mission provides a novel measurement tool that allows for the direct detection of changes in land water storage using satellite data [64–66]. In this study, we replaced WY with TWS in order to more accurately quantify the relationship between NPP and water.

In summary, although many scholars have conducted extensive research on vegetation NPP in the YRB, the selection of influencing factors is not comprehensive enough, and the use of water yield to study the mechanism of NPP changes is not accurate enough. Therefore, to comprehensively analyze the spatiotemporal changes in vegetation NPP in the YRB and systematically explore its mechanisms of change, this study is based on MODIS17A3 data, climate data, societal data, and GRACE data. It employs methods such as trend analysis, correlation analysis, and geographic detectors to analyze and explore the spatiotemporal evolution of vegetation NPP in the YRB from 2000 to 2022 and its influencing factors. The aim is to provide scientific references for the protection of the ecological environment and sustainable development in the YRB.

## 2. Data and Method

### 2.1. Study Area

The Yellow River is the second longest river and plays an important role in the ecosystem cycle in China. The landform in the region includes the Qinghai Tibet Plateau, the Inner Mongolian Plateau, the Loess Plateau, and the Huang Huai Hai Plain. The average altitude in the western region is over 4000 m, and the landforms are mostly high-altitude forests. The elevation of the central region is mostly between 1000 and 2000 m, with mostly forested and grassland landforms. However, soil erosion has been relatively severe throughout the year. The eastern region has a lower altitude and is mostly characterized by alluvial plains. The YRB belongs to a temperate monsoon climate, with significant seasonal climate changes and significant spatial differences (see Figure 1). It is an important ecological regulation system in China. In recent years, China has taken a series of environmental measures that have improved the ecosystem of the YRB [42,46,63]. Therefore, conducting a long-term assessment of the ecosystem in the YRB is extremely important. Based on this, this article focuses on exploring the spatiotemporal evolution characteristics and influencing factors of NPP in the YRB from 2000 to 2020.

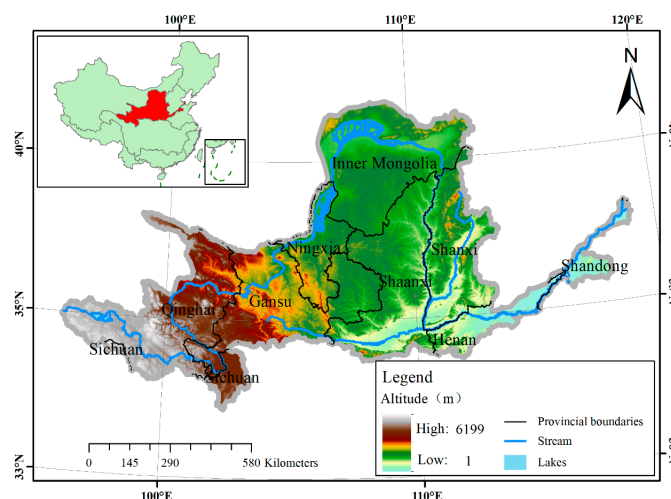


**Figure 1.** The Yellow River Basin (China) topography.

## 2.2. Data

This research used data that included NPP and multiple-factor data (Table 1) so we can explore the impact of various factors on NPP to the greatest extent possible. To facilitate the analysis, we categorize these factors into static and dynamic factors. Static factors encompass geographical location, elevation, slope, and soil type. Dynamic factors include meteorological factors (accumulated temperature, sunshine duration, temperature, and precipitation), TWS, and human activities (population density, GDP, and land use).

**Table 1.** The data used in this paper.

	Data	Period	Spatial Resolution	Website (Access Data: 30 December 2023)
Static factors	NPP	2000–2022	500 m	<a href="https://ladsweb.nascom.nasa.gov/">https://ladsweb.nascom.nasa.gov/</a>
	Geographical location			
	Elevation		1 km	<a href="http://www.Gscloud.cn">http://www.Gscloud.cn</a>
	Slope			
	Soil type			
Dynamic factors	Accumulated temperature			
	Sunshine duration	2000–2019	1 km	<a href="http://data.cma.cn/data">http://data.cma.cn/data</a>
	Temperature			
	Precipitation			
	TWS	2003–2019	0.25°	<a href="http://data.tpdc.ac.cn/data">http://data.tpdc.ac.cn/data</a>
	Land use			
	Population density	2000, 2005, 2010, 2015, 2019	1 km	<a href="http://www.resdc.cn">http://www.resdc.cn</a>
	GDP			

### 2.2.1. NPP

Remote sensing data is a crucial source of information for large-scale modeling and geoscientific research, offering advantages such as wide coverage, high resolution, and easy data acquisition. The vegetation NPP data is sourced from the MODIS17A3H dataset, covering the period from 2000 to 2022. The spatial resolution is 500 m, and the temporal resolution is 1 year. The valid value range is  $-3000$  to  $32700$ . First, the vegetation NPP data was preprocessed using the MODIS Reprojection Tools (MRT) tool to perform mosaicking and format conversion. Subsequently, ArcMap10.7 software was used to remove outliers from the NPP data, resample it to a 1 km resolution, and project it to the Krasovsky projection. At last, the processed NPP data was clipped to the study area.

### 2.2.2. Static Factors Data

Geographical location data, elevation data, and slope data can all be extracted using the SRTM90m dataset, which is sourced from the Geospatial Data Cloud Platform. This data is a joint measurement effort between NASA (National Aeronautics and Space Administration) and the National Geospatial-Intelligence Agency (NGA) of the Department of Defense. The spatial resolution is 90 m; we used ArcGIS to resample it to a 1 km resolution and project it to the Krasovsky projection.

### 2.2.3. Dynamic Factors Data

#### 1. Meteorological data

The meteorological data includes annual precipitation, annual mean temperature, annual accumulated temperature, and annual sunshine data from approximately 94 surface meteorological stations in the YRB. The data spans from 2000 to 2019, providing a total of 20 years' worth of data. The Kriging interpolation method available in the Geostatistical Analysis module of ArcGIS was utilized to generate this dataset. The resulting dataset has a spatial resolution of 1 km.

## 2. TWS data

The TWS data is from the “China Regional Land Water Storage Change Dataset Based on Precipitation Reconstruction (2002~2019)”, and the spatial resolution is 0.25°. Since the dataset contains some missing data for specific months that have not been interpolated, certain data processing is required. Firstly, the data in the dataset was arranged in a time series order according to their corresponding years and months. Months with complete data for the 18-year period from 2002 to 2019 were identified, excluding data from 2003 as it only has data from April onwards. The remaining excluded data includes monthly data from the years 2011, 2012, 2014, and 2015. The selected 13-year water storage data includes the same months of January, May, July, November, and December. Finally, since NPP data is annual data, the monthly data for water storage for the 13 years was averaged on an annual basis to obtain annual water storage data.

## 3. Human activity data

Population density and GDP are sourced from the Resource and Environment Science and Data Center. The spatial resolution of the data is 1 km, and the temporal resolution is 1 year. The data is in the Krasovsky projection coordinate system. The required data covers a period of 5 years (2000, 2005, 2010, 2015, and 2019). As there is a missing GDP data for 2020, the data from 2019 is used as a substitute. Land use data is also obtained from the Resource and Environment Science and Data Center. The data is in the Krasovsky projection coordinate system, with a spatial resolution of 30 m. ArcGIS was used to resample this data to a 1 km resolution. This dataset is created from Landsat remote sensing images and has been manually interpreted, providing a high level of data accuracy.

### 2.3. Method

#### 2.3.1. Miami Model

The Miami model is based on reliable measured data of NPP for the five major continents and matching data for annual mean precipitation and annual mean temperature. It is simulated through the establishment of a net productivity model using the least squares method. This model was originally designed and proposed by Lieth and is now widely applied in the estimation of the potential NPP of vegetation. The functional expression of this model is as follows:

$$NPP_c = \min\left\{\left(1 + \frac{3000}{\exp(1.315 - 0.119T)}\right), 3000[1 - \exp(-0.000664P)]\right\} \quad (1)$$

where  $NPP_c$  is the potential NPP ( $gC \cdot m^{-2} \cdot a^{-1}$ );  $T$  is the annual average temperature ( $^{\circ}C$ );  $P$  is the annual precipitation (mm).

#### 2.3.2. Trend Analysis

We use trend analysis to evaluate the intensity of vegetation NPP changes. This method can help eliminate the effects of extreme weather conditions in specific years [67–69]. The functional expression for this method is:

$$\theta_{\text{slope}} = \frac{n \times \sum_{i=1}^n i \times NPP_i - \sum_{i=1}^n i \sum_{i=1}^n NPP_i}{n \times \sum_{i=1}^n i^2 - \left(\sum_{i=1}^n i\right)^2} \quad (2)$$

where  $i$  represents the year;  $n$  is the number of years in the time series;  $NPP_i$  is the NPP for the  $i$ th year; and slope is the slope of the trend line, with positive or negative values indicating improvement or degradation trends in vegetation NPP over time. The following formula reveals the degree of vegetation NPP changes through the NPP change rate:

$$\beta = \frac{\theta_{\text{slope}}}{NPP_{\text{mean}}} \times 100\% \quad (3)$$

where  $\beta$  represents the vegetation NPP change rate and  $NPP_{\text{mean}}$  is the mean vegetation NPP.

### 2.3.3. Stability Analysis

The coefficient of variation (CV) is a common indicator that reflects sample fluctuations. Its value can reflect the stability of vegetation NPP in time series. The formula is as follows [70]:

$$C_v = \frac{1}{\bar{x}} \sqrt{\frac{\sum_{i=1}^n (x_i - \bar{x})^2}{n-1}} \quad (4)$$

where  $C_v$  is the coefficient of variation. The smaller the value, the more stable the vegetation NPP is in the time series.  $x_i$  is the NPP value of the  $i$ -th year;  $\bar{x}$  is the average of NPP in  $n$  years.

### 2.3.4. Geographical Detector

The Geographical Detector, which is proposed by Wang, is an analytical model used to detect and utilize spatial variations [70]. The Geographical Detector model can reveal the explanatory power of a certain factor on vegetation NPP [71]. The  $q$ -value represents the degree of influence:

$$q = 1 - \frac{\sum_{h=1}^L N_h \sigma_h^2}{N \sigma^2} = 1 - \frac{SSW}{SST} \quad (5)$$

$$SSW = \sum_{h=1}^L N_h \sigma_h^2 \quad (6)$$

$$SST = N \sigma^2 \quad (7)$$

where  $h = 1, \dots, L$  is the NPP influencing factors;  $N_h$  and  $N$  are the number of units in layer  $h$  and the entire area, respectively;  $\sigma_h^2$  is the variance of the class  $h$ ;  $\sigma^2$  is the variance for the entire region;  $SSW$  is the sum of variances within the layer; and  $SST$  is the total variance of the entire region.

### 2.3.5. Transfer Matrix

A transfer matrix is used to reflect the transfer situation between NPPs of different levels of vegetation [31]. The expression is:

$$S_{i,j} = \begin{pmatrix} S_{11} & \cdots & S_{1n} \\ \vdots & \ddots & \vdots \\ S_{n1} & \cdots & S_{nn} \end{pmatrix} \quad (8)$$

where  $S$  represents the transfer area ( $\text{km}^2$ ) of different levels;  $n$  represents different vegetation NPP levels;  $i, j$  represent the vegetation NPP levels in the initial period and the final period, respectively; and  $S_{nn}$  represents the area change of vegetation NPP levels from the initial period to the final period ( $\text{km}^2$ ).

## 3. Results and Analysis

This section is divided into three parts, namely, the spatiotemporal distribution characteristics of vegetation NPP, the static factors analysis, and the dynamic factors analysis.

### 3.1. Spatiotemporal Distribution Characteristics of Vegetation NPP in the Yellow River Basin

In this part, we separately counted the spatiotemporal changes of NPP and analyzed the rate of change and stability.

### 3.1.1. Spatiotemporal Changes in Vegetation NPP in the Yellow River Basin from 2000 to 2022

To investigate the overall spatial distribution of vegetation NPP in the YRB, we calculated the average spatial distribution of NPP from 2000 to 2022 (Figure 2a) and the area proportions of different NPP categories (Figure 2b). The spatial distribution of vegetation NPP in the YRB is highly uneven, showing significant variations. The specific characteristics include the following: (1) Elevation variation—the vegetation NPP is lower in the northwest region and increases towards the southeast. (2) Numerical range is large, from 0 to 1077  $\text{gC}\cdot\text{m}^{-2}\cdot\text{a}^{-1}$ . According to statistics, the value of NPP is generally between 0 and 800  $\text{gC}\cdot\text{m}^{-2}\cdot\text{a}^{-1}$ . Therefore, in order to analyze the changes in NPP in detail, we use the equal interval classification method to divide NPP into five levels—low ( $<200 \text{ gC}\cdot\text{m}^{-2}\cdot\text{a}^{-1}$ ), lower (200–400  $\text{gC}\cdot\text{m}^{-2}\cdot\text{a}^{-1}$ ), median (400–600  $\text{gC}\cdot\text{m}^{-2}\cdot\text{a}^{-1}$ ), higher (600–800  $\text{gC}\cdot\text{m}^{-2}\cdot\text{a}^{-1}$ ), and high ( $>800 \text{ gC}\cdot\text{m}^{-2}\cdot\text{a}^{-1}$ ). (3) Area distribution—the low NPP area accounts for 31.59% and is mainly found in western Sichuan and the northern regions of Gansu, Ningxia, and Inner Mongolia. The lower NPP area accounts for 46.96% and is mainly located in Qinghai, the northern part of the Loess Plateau, and the middle and lower reaches of the Yellow River. The median NPP area accounts for 19.88% and is mainly found at the border of Shaanxi, Shanxi, and Henan. The higher and higher NPP areas account for approximately 1.57% and are concentrated in the Guanzhong Plain, south of the Weihe River.

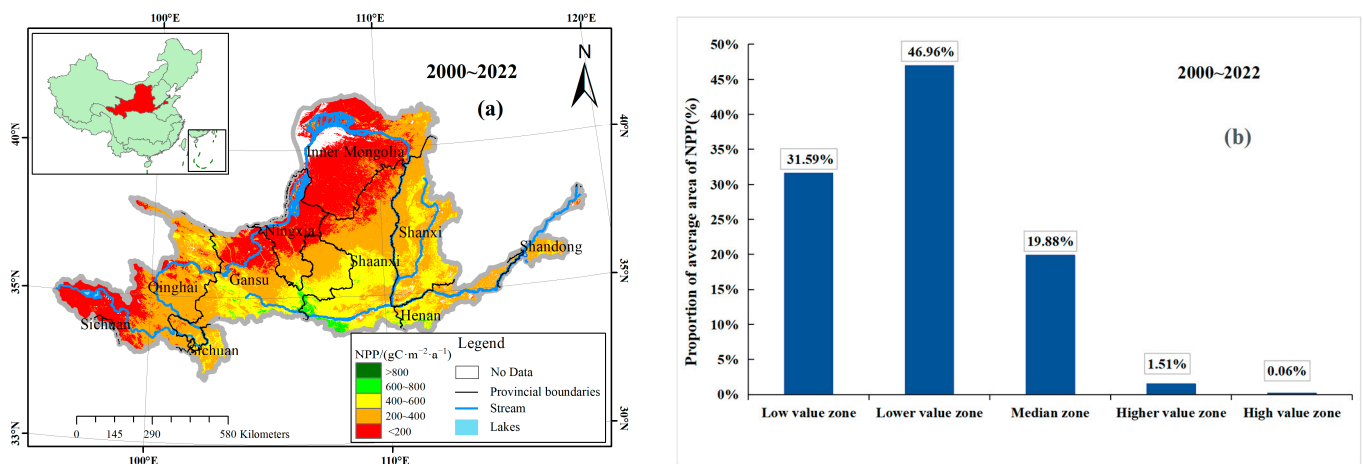


**Figure 2.** Spatial Distribution of Vegetation NPP in YRB from 2000 to 2022 (NPP divided into five categories based on numerical values). (a) shows the spatial distribution of different NPP levels in YRB; (b) right side shows the area proportion of different NPP levels in YRB.

After understanding the average distribution of vegetation NPP in the YRB, we analyzed the spatiotemporal changes in vegetation NPP from 2000 to 2022 (Figure 3). The spatial map (Figure 3a) shows an overall increase in vegetation NPP in most regions of the YRB, except for the western and northern areas, which exhibit a decrease in vegetation NPP. The average annual time series of vegetation NPP in the YRB (Figure 3b) also indicates a consistent annual increase since 2000. Table 2 provides statistics on the area proportions of different NPP categories and the overall change ratio for 2000 and 2022, offering a more precise representation of the characteristics of vegetation NPP changes. The results show that the areas of low and lower NPP have decreased, particularly the low NPP area, which has reduced by half, accounting for one-fourth of the entire Yellow River Basin area. The median NPP area has increased by more than ten times, equivalent to about one-fourth of the basin area. To more accurately assess the transitions between NPP categories over a decade, we calculated the NPP transition matrices (Figure 4) and compiled spatial change maps (Figure 5). From 2000 to 2010, approximately 59.75% of the areas maintained the same category. Low NPP areas transitioned to lower NPP areas (about 20.09%), and lower NPP areas changed to median NPP areas (about 15.44%), mainly in the southern part of the middle Yellow River Basin. Transitions from median NPP to higher NPP areas accounted

for about 1.32% and were concentrated in the plain areas along the southern bank of the Weihe River. From 2010 to 2022, approximately 68.34% of the areas retained their NPP categories, primarily in the entire northwest region of the YRB. Areas transitioning from lower NPP to median NPP comprised about 17.45%, forming strip-like patterns along both sides of the middle and lower reaches of the Yellow River. Transitions from median NPP to higher NPP areas accounted for about 4.31%, mainly distributed in various tributary regions in central Shaanxi, while transitions between other categories were relatively minor.

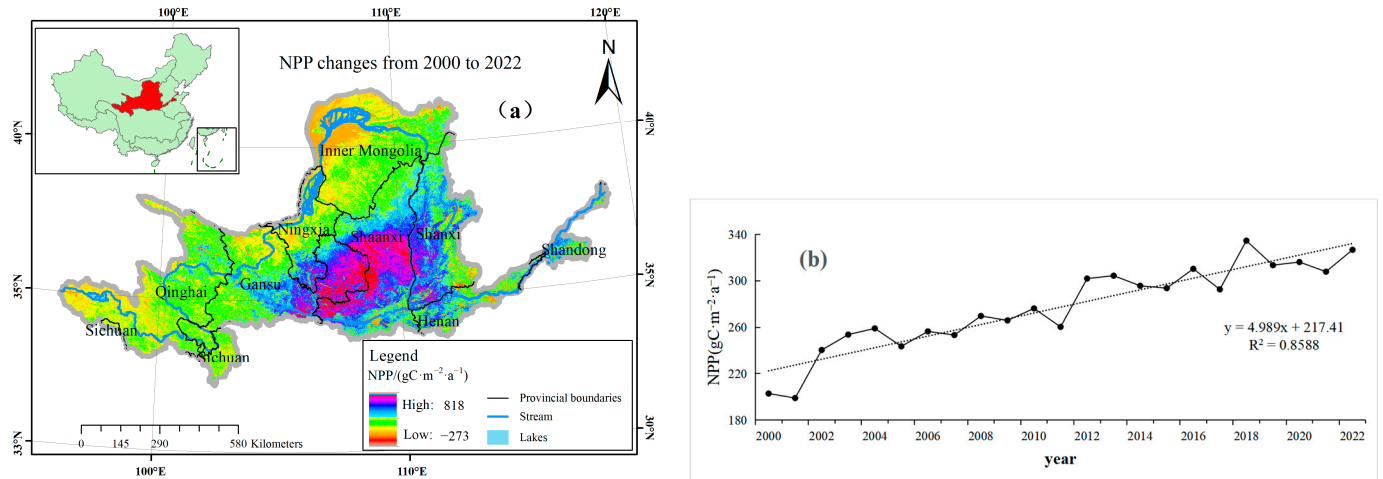


**Figure 3.** Spatiotemporal changes in vegetation NPP in YRB from 2000 to 2022 ((a) shows the spatial changes, (b) shows the temporal changes).

**Table 2.** Summary of changes in area proportion of each level of vegetation NPP in YRB from 2000 to 2022.

NPP ( $\text{gC}\cdot\text{m}^{-2}\cdot\text{a}^{-1}$ )	NPP Categories	Area Ratio (2000)	Area Ratio (2022)	Area Ratio Change (2000–2022)
<200	Low	53.42%	27.98%	−25.44%
200~400	Lower	41.62%	35.49%	−6.13%
400~600	Median	2.60%	30.84%	28.24%
600~800	Higher	2.35%	5.59%	3.24%
>800	High	0.01%	0.10%	0.09%

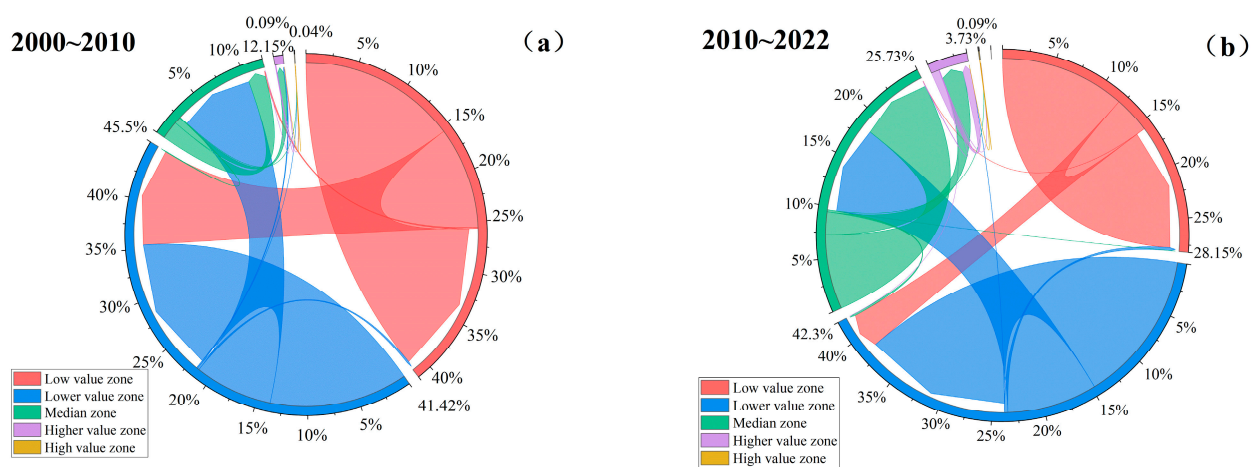


**Figure 4.** Chord chart (area proportion) of vegetation NPP level conversion in different periods of YRB ((a) 2000–2010; (b) 2010–2022).



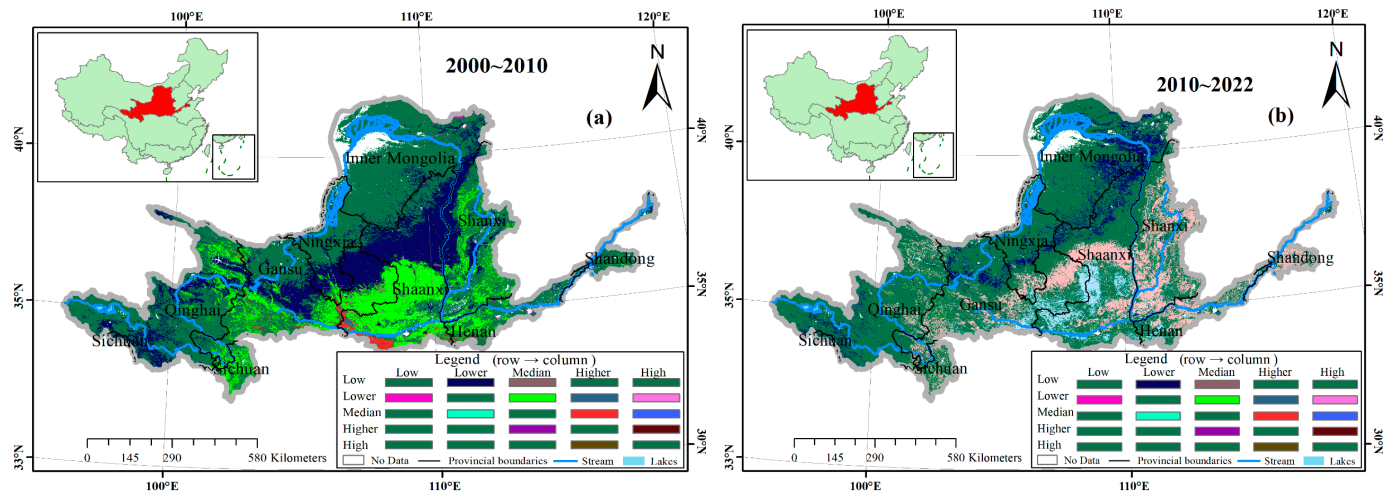


**Figure 5.** NPP level transfer diagram in different periods of YRB ((a) 2000–2010; (b) 2010–2022).

In summary, considering vegetation NPP as an indicator of ecological assessment, it is evident that over the past two decades, areas with extreme degradation have significantly decreased in the YRB. With the exception of the western Sichuan region and the northern regions of Gansu, Ningxia, and Inner Mongolia, low NPP areas are transitioning to lower NPP areas, lower NPP areas are transitioning to median NPP areas, and the higher NPP areas continue to increase. This indicates substantial improvement in the ecological environment.

### 3.1.2. Change Rate and Stability Analysis

To gain a more precise understanding of the NPP changes and to assess the ecological changes in the region, we calculated the vegetation NPP change rates from 2000 to 2022 and classified them (Figure 6). According to the amplitude of change, classify them evenly, including Substantial Decrease Zone ( $< -10$ ), Moderate Decrease Zone ( $> -10, < 0$ ), Moderate Increase Zone ( $> 0, < 10$ ), Significant Increase Zone ( $> 10, < 20$ ), High Increase Zone ( $> 20, < 30$ ), and Very High Increase Zone ( $> 30$ ). The results indicate that from 2000 to 2022, areas with increased vegetation cover in the YRB accounted for 98.52% of the entire region. Among these, the high increase zone covered 67.45% of the total area, primarily located in the central part of the YRB and the Loess Plateau region. This suggests that these areas have experienced the most significant ecological improvement. The moderately high and moderate increase zones covered 25.24% of the total area and were mainly distributed in the southern parts of Sichuan and Qinghai, indicating that high-altitude regions have undergone some degree of ecological restoration.

The coefficient of variation is a measure used to assess the degree of variability in data. In general, a larger coefficient of variation indicates greater variability in the data. To evaluate the stability of vegetation NPP changes in the YRB, we introduced the coefficient of variation (Figure 7). The coefficient of variation for vegetation NPP in the YRB ranged from 0.04 to 1.42. According to statistics, the majority of NPP changes are concentrated between 0.1 and 0.4. In order to analyze NPP changes in detail as much as possible, we categorized it into five levels ( $< 0.1$ ,  $0.1-0.2$ ,  $0.2-0.3$ ,  $0.3-0.4$ , and  $> 0.4$ ). Overall, across the entire Yellow River Basin, there is an increasing trend in the coefficient of variation of vegetation NPP from the outer regions towards the inner regions. This trend suggests that vegetation NPP experiences more frequent and dramatic changes in the inner regions of the YRB, particularly in the Loess Plateau in the central part.

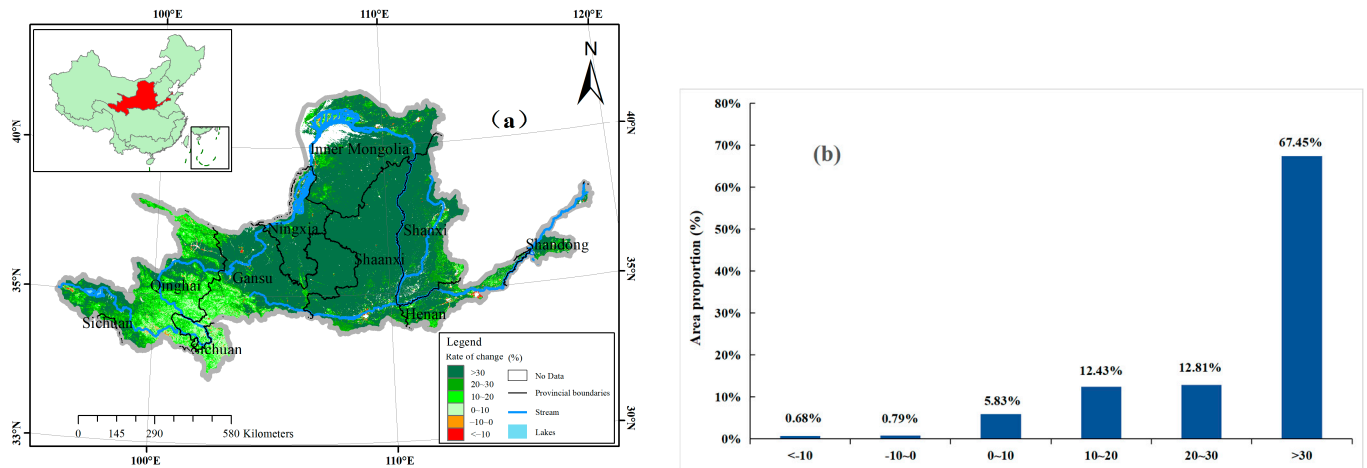


**Figure 6.** Analysis results of NPP change rate of vegetation in YRB ((a) spatial distribution of NPP change rate of vegetation in YRB; (b) statistical chart of NPP change rate of vegetation in YRB).

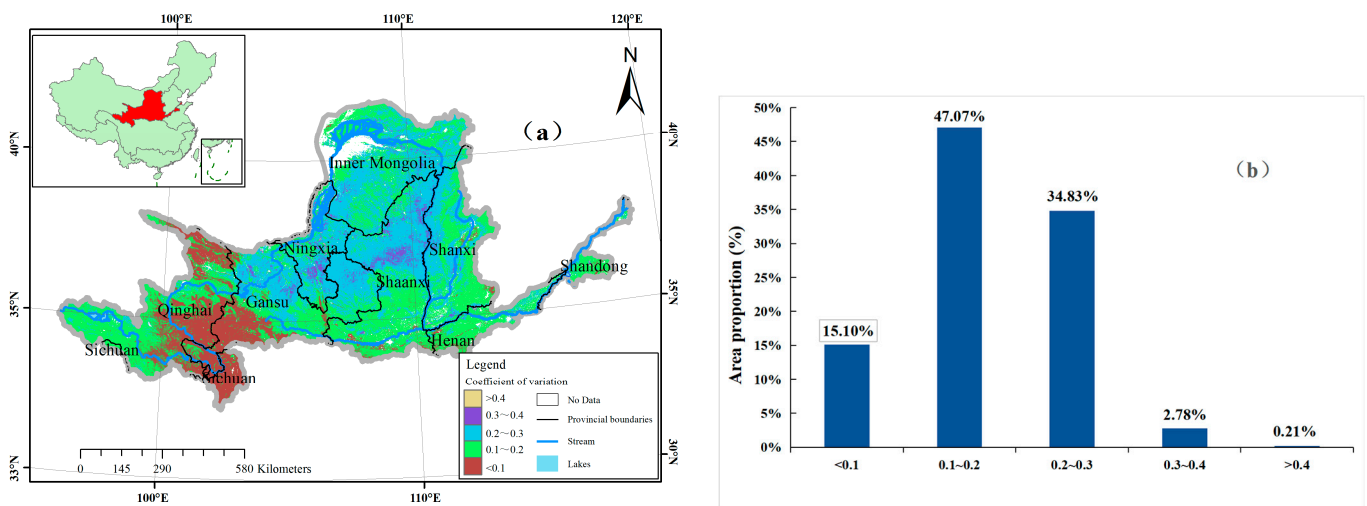


**Figure 7.** NPP stability analysis results of vegetation in YRB ((a) spatial distribution of NPP variation coefficient of vegetation in YRB; (b) statistical chart of NPP variation coefficient of vegetation in YRB).

### 3.2. Static Factors Analysis on Vegetation NPP in the YRB

We analyzed the correlation between static factors (geographic location, elevation, and slope) and changes in NPP separately.

#### 3.2.1. Geographical Location Analysis on Vegetation NPP in the YRB

YRB covers a vast geographic area, and it is essential to analyze the impact of geographical location on vegetation NPP. This analysis involves categorizing the region based on longitude (108° E and 111° E) and latitude (34.42° N and 36.5° N), as shown in Figure 8.

From Figure 8, we can see that NPP varies greatly in different geographical locations. In the overall distribution, vegetation NPP tends to be higher in the southern part of the YRB compared to the northern part and higher in the eastern regions compared to the western regions. At the same latitude, with increasing longitude, vegetation NPP generally follows a pattern of increase, decrease, and then increase again. When we move eastwards into the heart of the Loess Plateau and the plain areas around the Wei River, NPP reaches its maximum. Further eastward, NPP becomes more stable. On the other hand, at the same longitude, there is an overall decreasing trend in vegetation NPP. This analysis provides valuable insights into how geographical location impacts vegetation NPP within the YRB.

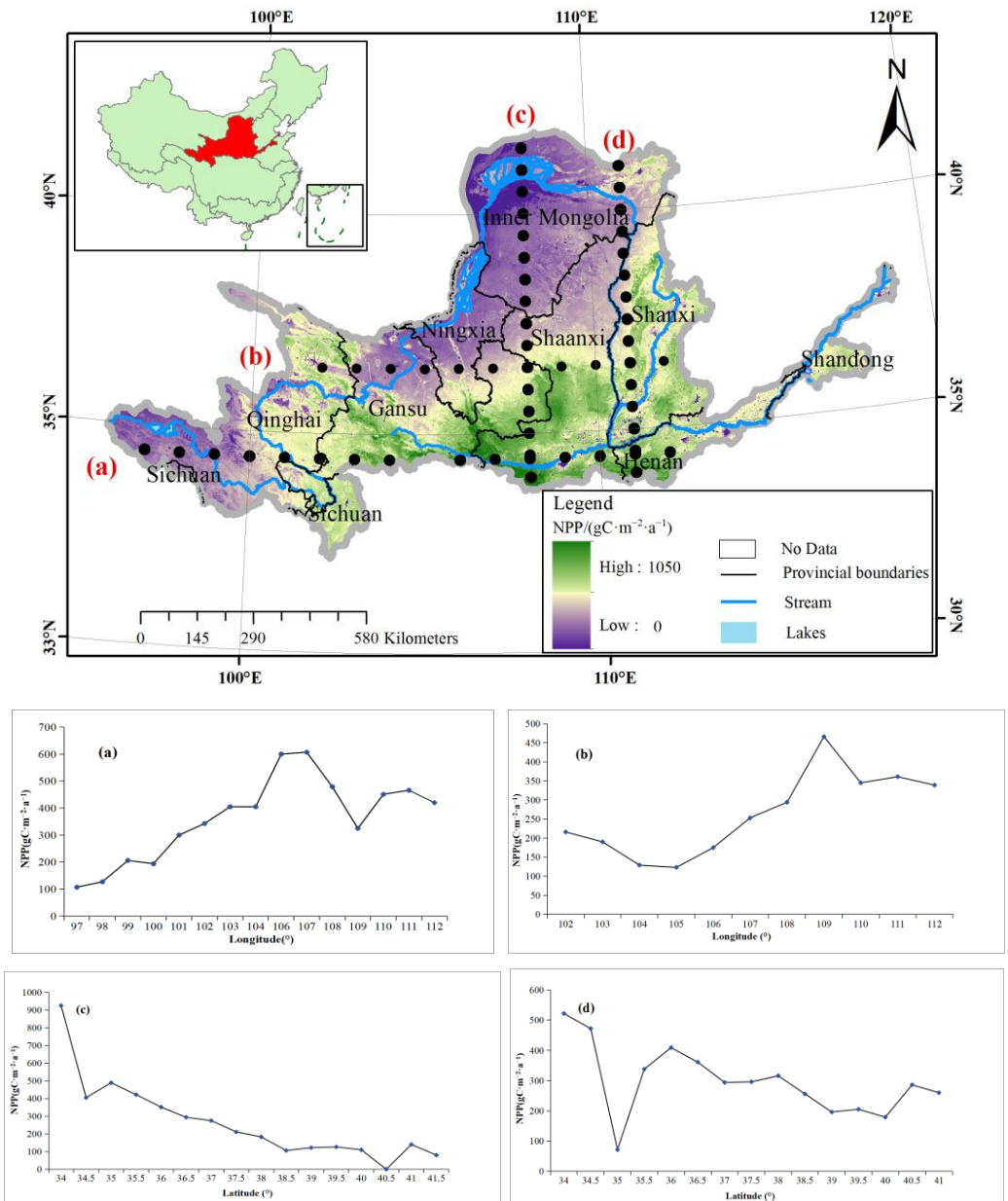


**Figure 8.** Spatial map of vegetation NPP in typical longitude and latitude areas ((a) vegetation NPP point value map from west to east along latitude 34.42° N; (b) vegetation NPP point value map from west to east along latitude 36.5° N; (c) vegetation NPP point value map from south to north along 108° longitude; (d) vegetation NPP point value map along 111° longitude from south to north).

### 3.2.2. Altitude Analysis on Vegetation NPP in the YRB

YRB exhibits significant variations in elevation, ranging from 0 to 6199 m. It is essential to analyze the impact of elevation on vegetation NPP within the YRB. To conduct this analysis, we categorized elevations into five classes using equal intervals: low elevation (<1000 m), low-medium elevation (1000–2000 m), medium elevation (2000–3000 m), medium-high elevation (3000–4000 m), and high elevation (>4000 m). Based on this classification method, we conducted a statistical analysis of vegetation NPP data, as shown in Figure 9 and Table 3.

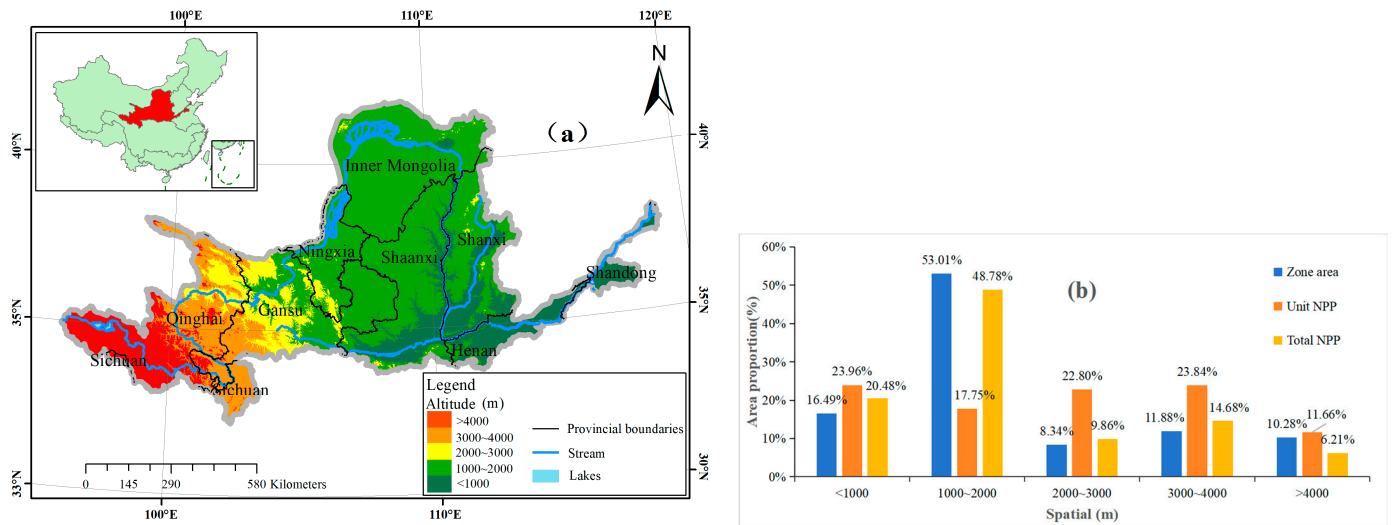


**Figure 9.** Statistical map of elevation divisions and vegetation NPP in YRB ((a) spatial distribution map of divisions according to altitude in YRB; (b) the proportion of NPP area divided by altitude in YRB).

**Table 3.** NPP statistics of vegetation in different altitude zones.

Spatial (m)	Spatial Proportion (%)	Unit NPP ( $\text{gC}\cdot\text{m}^{-2}\cdot\text{a}^{-1}$ )	RMS ( $\text{gC}\cdot\text{m}^{-2}\cdot\text{a}^{-1}$ )	Unit NPP Proportion (%)	Total NPP ( $\text{gC}\cdot\text{m}^{-2}\cdot\text{a}^{-1}$ )	Total NPP Proportion (%)
<1000	16.49%	344.37	122.68	23.96%	56.79	20.48%
1000~2000	53.01%	255.14	152.37	17.75%	135.25	48.78%
2000~3000	8.34%	327.68	148.4	22.80%	27.33	9.86%
3000~4000	11.88%	342.62	77.33	23.84%	40.70	14.68%
>4000	10.28%	167.55	75.94	11.66%	17.22	6.21%

The results indicate that the YRB’s low and low-medium elevation areas have the largest proportion, accounting for 69.50%. These areas are primarily concentrated in the middle and lower reaches of the Yellow River, while the upper reaches of the Yellow River are generally at medium elevation and above. The unit NPP (NPP per unit area) is relatively high in the low-elevation, medium-elevation, and medium-high-elevation regions, all exceeding 20%. These areas are mainly found in the belt regions on both sides of the middle and lower reaches of the Yellow River. This suggests that a combination of factors, including climate and other conditions, favors plant growth in these regions. It is worth noting that in the hinterland of the middle reaches of the YRB, which includes the Loess Plateau, although the altitude is relatively low, the unit NPP is relatively low. But looking at the total NPP, YRB’s vegetation NPP is mainly concentrated in the low and low-medium elevation areas, primarily due to the larger area proportion these elevations occupy.

### 3.2.3. Slope Analysis on Vegetation NPP in the YRB

The terrain of the YRB is complex. In order to study the impact of terrain on vegetation NPP, we use slope as an indicator and divide the slope into five levels on average based on the magnitude of the slope values in the region. We then analyzed the NPP values corresponding to these different slope categories, as shown in Figure 10 and Table 4. The results reveal that the majority of the YRB’s regions have slopes of  $6^\circ$  or less (88.74%), covering almost the entire basin except for mountainous areas in the western and southern regions. A general trend is observed when considering unit NPP (NPP per unit area), where higher slopes are associated with higher unit NPP. But, due to the distribution of slope categories in the YRB, the total vegetation NPP is primarily concentrated in areas with lower slopes ( $<6^\circ$ ), accounting for 86.18% of the total NPP.

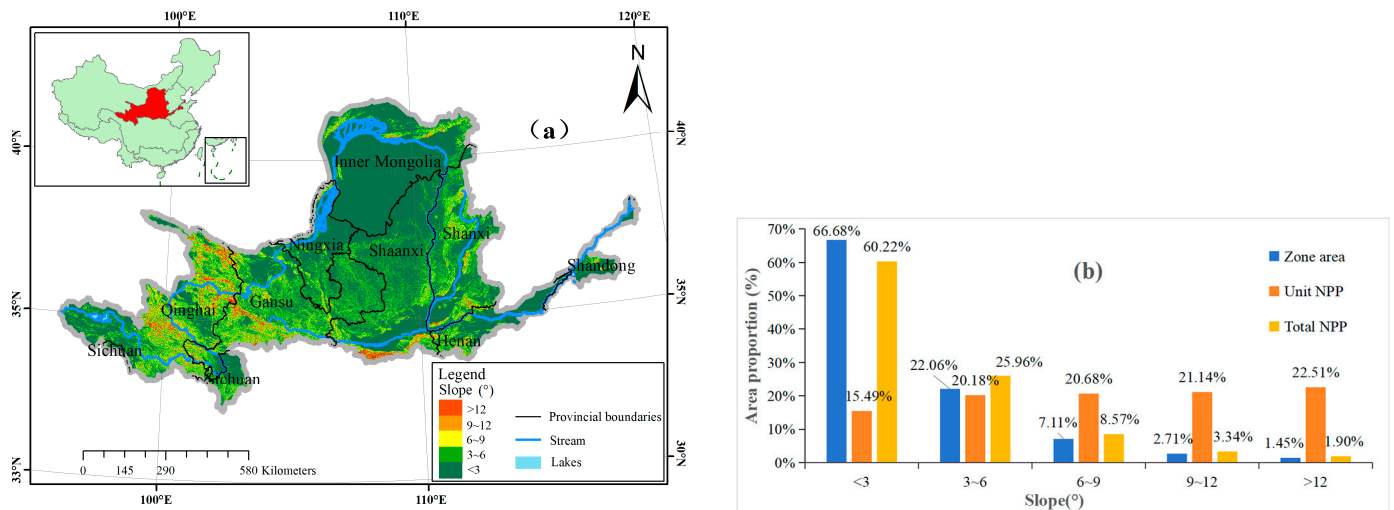


**Figure 10.** Slope classification of YRB ((a) slope grading plan of YRB; (b) proportion of NPP with different slope grades in YRB).

**Table 4.** NPP statistics of vegetation on different slopes.

Slope (°)	Slope Proportion (%)	Unit NPP (gC·m <sup>-2</sup> ·a <sup>-1</sup> )	RMS (gC·m <sup>-2</sup> ·a <sup>-1</sup> )	Unit NPP Proportion (%)	Total NPP (gC·m <sup>-2</sup> ·a <sup>-1</sup> )	Total NPP Proportion (%)
<3	66.68%	250.46	138.1	15.49%	167.01	60.22%
3~6	22.06%	326.39	136.12	20.18%	72.00	25.96%
6~9	7.11%	334.43	146.67	20.68%	23.78	8.57%
9~12	2.71%	341.94	156.84	21.14%	9.27	3.34%
>12	1.45%	364.02	170.83	22.51%	5.28	1.90%

### 3.3. Dynamic Factors Analysis Analysis on Vegetation NPP in the YRB

In order to comprehensively analyze the relationship between dynamic factors and NPP changes, we focused on the correlation between NPP and climate factors (accumulated temperature, sunlight, precipitation, and temperature), as well as water reserves. In addition, we selected nine factors for single-factor analysis with NPP.

#### 3.3.1. Correlation Analysis on Vegetation NPP in the YRB

NPP in the YRB is closely related to climate factors, including accumulated temperature, sunshine duration, precipitation, and temperature. Based on this foundation, we also considered TWS in our analysis. We calculated the correlation coefficients between these factors and NPP and then examined the area percentages for different scenarios (as shown in Figures 11 and 12 and Table 5). We found the following relationships: The same trend as the NPP of vegetation in the YRB is accumulated temperature, precipitation, and temperature, while the opposite is sunshine and TWS.

Accumulated temperature is closely related to the development of organic organisms, and it has a positive impact on NPP. It was found to be positively correlated with NPP in 87% of the YRB. The impact of accumulated temperature is closely related to elevation, with a significant influence in higher elevation areas, such as Qinghai, Sichuan, and the southwestern part of Gansu. This suggests that accumulated temperature is an important factor in NPP changes in high-elevation regions where external factors vary less.

NPP and sunshine duration are mostly negatively correlated (64%), particularly in the central part of the YRB, including Gansu, Ningxia, and Shaanxi. Positive correlations were mainly observed in areas adjacent to the middle and lower reaches of the Yellow River. Comparison with the slope classification map indicates that the impact of sunshine duration on NPP in the YRB is closely related to topography. Positive correlation areas are mainly distributed in areas with smaller slopes.

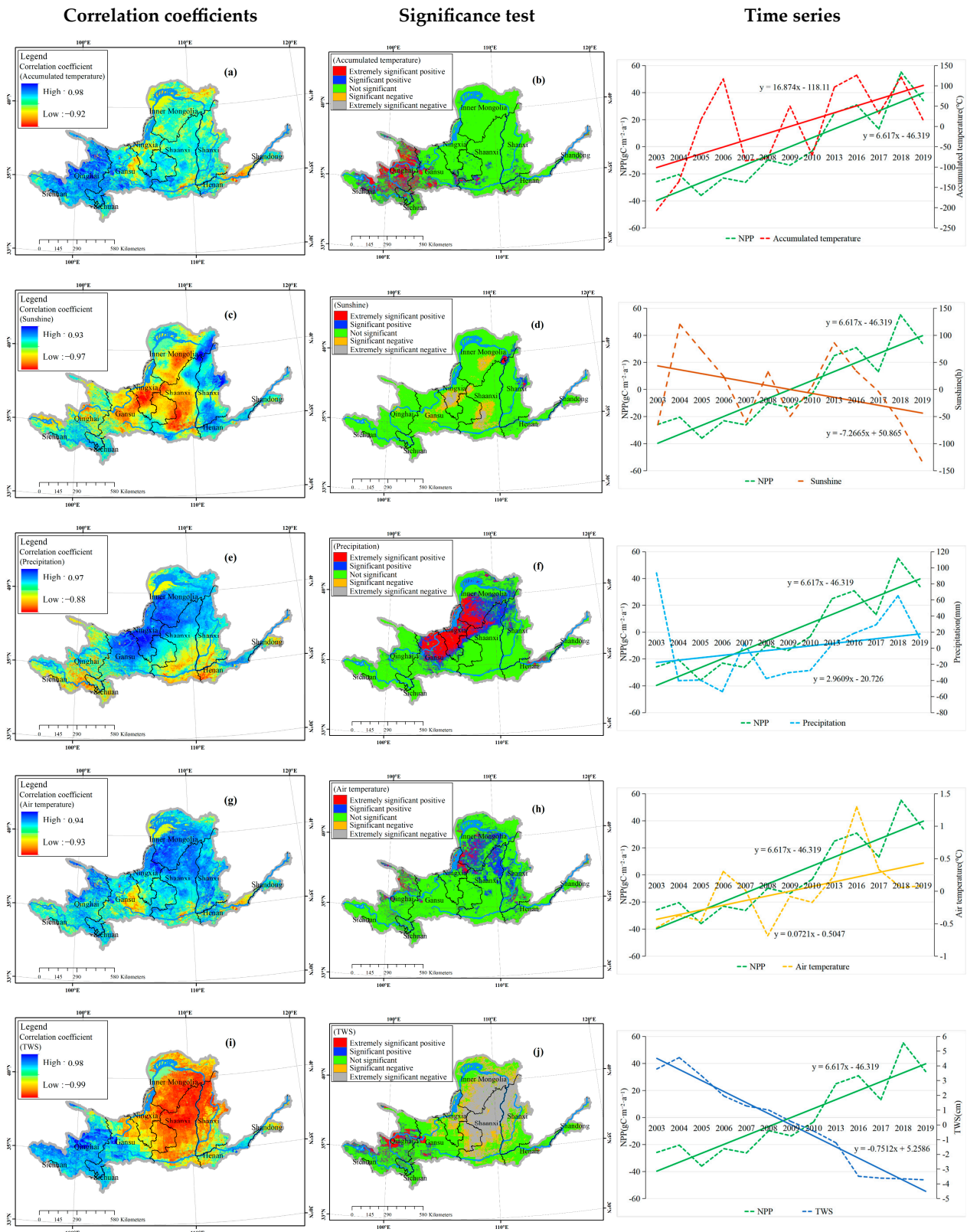


**Figure 11.** Spatial distribution and time series map of correlation analysis between vegetation NPP and five factors in YRB. (a,c,e,g,i) are the spatial distribution map of correlation coefficients between NPP and five factors (accumulated temperature, sunlight, precipitation, temperature, and TWS) in YRB; (b,d,f,h,j) are the spatial distribution map of significance test between NPP and five factors in YRB; the solid line represents the time series, and the dashed line represents the linear trend.

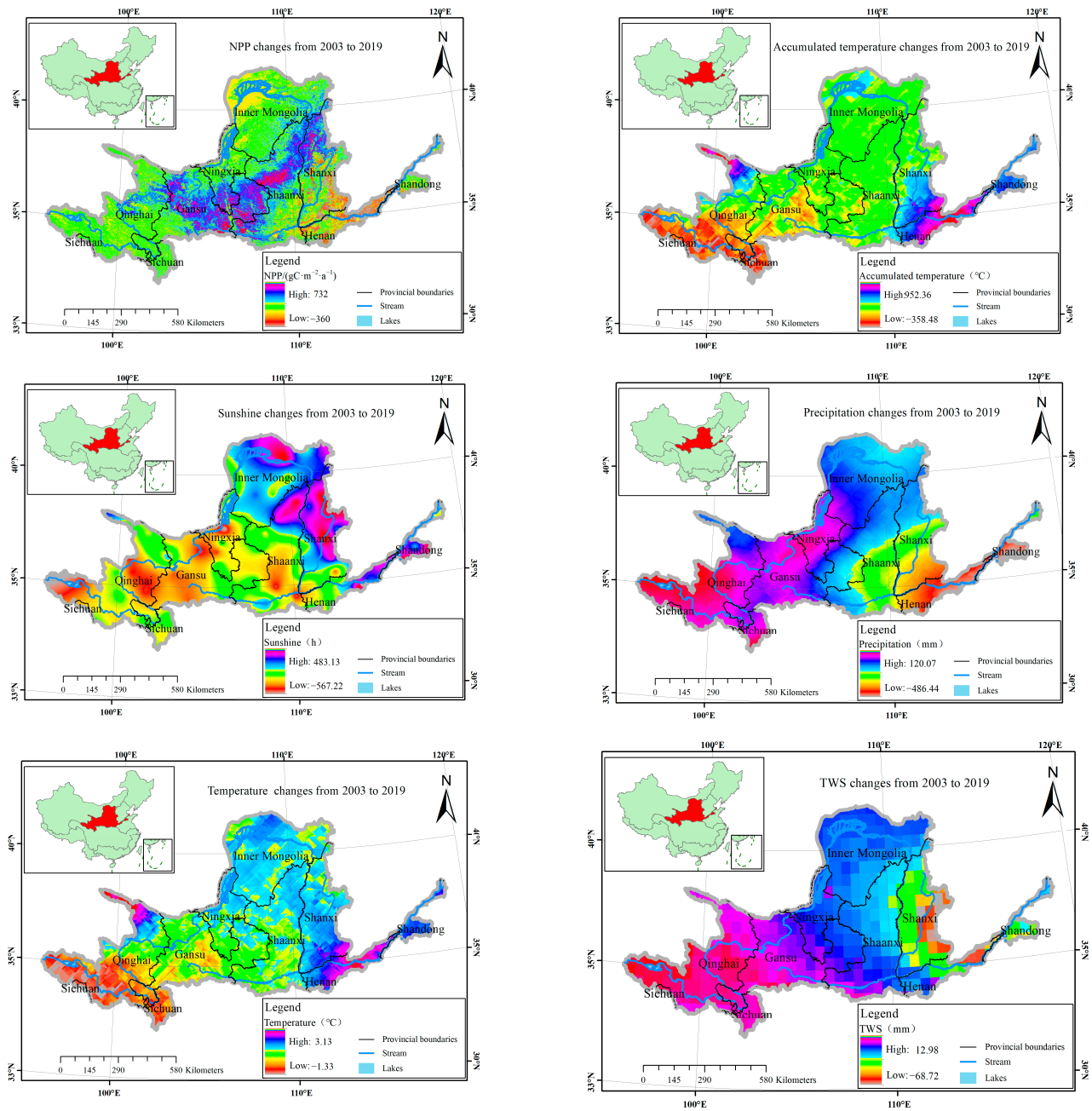


**Figure 12.** The spatial distribution of vegetation NPP in YRB from 2003 to 2019.

NPP and precipitation are positively correlated in most regions (81%), predominantly in the northern part of the YRB, such as Gansu, Ningxia, and Inner Mongolia, which are part of the Loess Plateau. This indicates that precipitation is one of the main factors promoting vegetation growth in these areas. Notably, along the Yellow River's south bank in Henan, the correlation between precipitation and NPP is low.

NPP and temperature exhibit a positive correlation in approximately 89% of the YRB, with a significant impact in various provinces and regions, particularly in Qinghai and Sichuan. A negative correlation was observed in about 11% of the area, with eastern Henan showing the most significant negative correlation.

NPP and TWS are positively correlated in about 32% of the area, mainly in the western part of the YRB, including Sichuan, Qinghai, Gansu, and the eastern part of Henan. The negative correlation accounts for approximately 67% of the area, nearly twice the positive

correlation area. This concentration is in the middle and lower reaches of the YRB, where NPP growth is fastest.

**Table 5.** Summary table of correlation area proportion between vegetation NPP and five factors in YRB.

Correlation Coefficient	Correlation	Area Proportion				
		Accumulated Temperature	Sunshine	Precipitation	Air Temperature	TWS
−1~−0.8	Negative extremely strong	0%	0%	0%	0%	16%
−0.8~−0.6	Negative strong	0%	6%	0%	0%	19%
−0.6~−0.4	Negative moderate	1%	15%	1%	1%	13%
−0.4~−0.2	Negative weak	2%	20%	4%	2%	8%
−0.2~−0	Negative extremely weak	11%	23%	14%	9%	11%
0~0.2	Positive extremely weak	18%	17%	15%	13%	7%
0.2~0.4	Positive weak	32%	12%	18%	28%	9%
0.4~0.6	Positive moderate	20%	6%	25%	36%	10%
0.6~0.8	Positive strong	15%	1%	20%	12%	5%
0.8~1	Positive extremely strong	2%	0%	3%	0%	1%
Average proportion		31%	17%	35%	34%	39%
Significance proportion (>95%)		76.42%	85.75%	50.95%	87.21%	52.48%
Linear trend (npp:6.617)		16.874	−7.2665	2.9609	0.0721	−0.7512
Linear correlation coefficient with NPP		0.58	−0.27	0.45	0.55	−0.89

To quantitatively assess the mutual interactions between NPP and these five factors in the YRB, we analyzed different levels of correlation, which provided an assessment of the extent to which each factor affects NPP. Based on the results in Table 5, the importance of these factors on NPP in the YRB, in descending order, is TWS, precipitation, temperature, accumulated temperature, and sunshine duration. These factors exhibited high reliability (over 95%), with areas exceeding 50%.

Through linear correlation analysis (in this linear trend analysis, incomplete data may lead to certain errors in the results, which will be discussed in Part 4), it was found that from the average change of 13 years, the same trend as the vegetation NPP in the YRB is accumulated temperature, precipitation, and temperature, while the opposite trend is sunshine and TWS. From the linear correlation coefficient, the strongest correlation with vegetation NPP change is TWS, temperature, accumulated temperature, and precipitation.

Therefore, overall, changes in TWS cannot be overlooked in the assessment of factors affecting NPP in the YRB.

### 3.3.2. Single Factor Analysis on Vegetation NPP in the YRB

In order to comprehensively analyze the contribution of various factors to the changes in vegetation NPP in the YRB, based on the conclusions from earlier discussions, we selected nine factors for comprehensive assessment. These factors include two climate-related factors, temperature, and precipitation, as well as land water storage, population density, GDP factors, two topographical factors, elevation and slope, and two land-related factors, land use and soil type. Considering data availability and the need for a detailed analysis of the impact of each factor, we used a geographic detector to calculate the contribution rates for different factors for the years 2000, 2005, 2010, 2015, and 2020 to evaluate the influence of different factors on NPP (as shown in Figure 13).

Looking at the five-year average contribution rates, soil type (0.48), precipitation (0.46), and temperature (0.32) had the most significant impact on vegetation NPP in the YRB. The next is land use (0.28), elevation (0.14), slope (0.12), and TWS (0.12), the added factor in this study. This suggests that topographical factors also influence vegetation NPP, although their impact is lower than climate and land factors. It also emphasizes the importance of water storage when assessing changes in vegetation NPP in the YRB. Finally, the social factors of GDP (0.02) and population density (0.01) had the least impact. This indicates



that, at present, societal activities have minimal influence on the overall changes in NPP in the YRB.

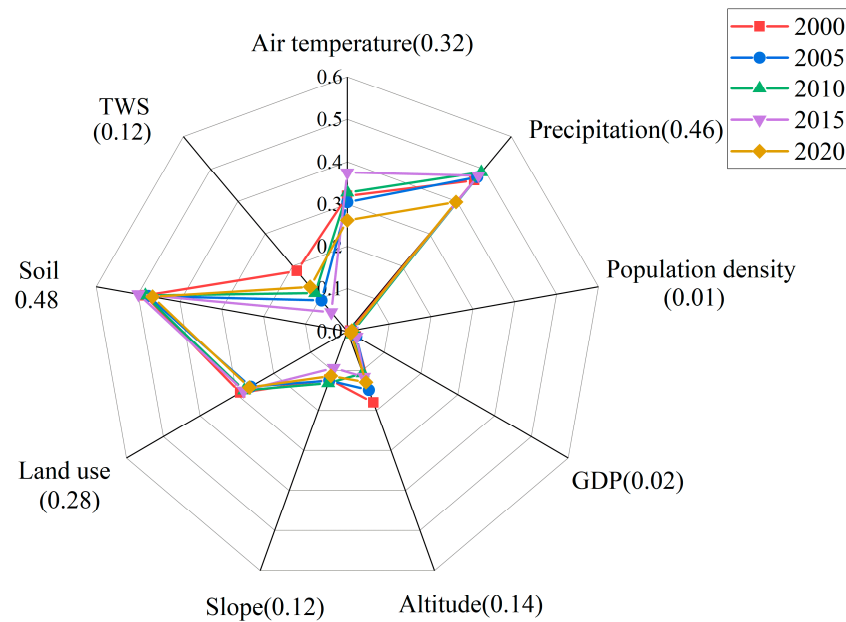


**Figure 13.** Contribution rate of various factors to changes in vegetation NPP in YRB (q-value).

#### 4. Discussion

This study is based on various datasets and explores the spatiotemporal changes in vegetation NPP in the YRB over a span of 23 years while quantifying the underlying influencing factors. To understand the influencing factors of vegetation NPP in the YRB as accurately as possible, we categorized the influencing factors into static and dynamic categories. Notably, this study is the first to include water storage as a factor in the analysis of the spatiotemporal changes in vegetation NPP in the YRB. The overall results indicate an increasing trend in vegetation NPP, signifying an improvement in the ecological environment. This conclusion has also been verified in relevant articles; NPP is increased in the upstream [47,50,54–56,61,62], in the total basin [28,46,63], in the middle reaches [51,57,58,71], and in the downstream [43]. In our exploration of the influencing factors underlying the changes in NPP in the YRB, we have reached conclusions similar to those of other studies. The correlation analysis results indicate that precipitation [42,46,51,56,57,63] and temperature [46,51,55,57] are the main factors affecting vegetation NPP. In addition, we found that TWS is also one of the main factors affecting NPP changes. Among the nine single-factor analyses, we also obtain the results that have been validated in other studies; soil type [48], precipitation, and temperature have the most significant impact, followed by land use [51,63,72], and then elevation [42,67], slope [42,62], and the newly added TWS factor, each with a five-year average contribution rate of 0.12. This highlights the importance of the TWS factor when assessing changes in vegetation NPP in the YRB. But, this study has a few points that need discussion.

In the analysis and conclusion of the NPP spatiotemporal changes, for the convenience of analysis, we classified NPP levels and calculated the average distribution of each level and the 23-year changes. Through the NPP mean map of the YRB for 23 years (2000–2020), we found that the spatial distribution of vegetation NPP in the YRB is extremely uneven, showing significant differences. In order to quantify the changes in vegetation NPP in the YRB, we calculated the proportion of vegetation NPP areas at different levels in 2000 and 2022 and obtained the changes. Although we used values from the first and last years of the study period, the overall changes from the beginning to the end can be obtained, but the changes in the middle of the period were not accurately measured. After considering this issue, we divided the research period into ten years (2000–2010, 2010–2022) and calculated

the changing area of vegetation NPP at each level. The overall results showed that the vegetation NPP in the YRB was transitioning from low to high levels. However, there are significant differences in changes between the two ten-year periods, so it is necessary to refine the research period of vegetation NPP in the YRB in the future. In order to gain a more accurate understanding of the changes in vegetation NPP in the YRB, we calculated the change rates of vegetation NPP at different levels from 2000 to 2022 in order to obtain the changes in vegetation NPP in each region. Finally, we use the coefficient of variation to value the severity of changes in vegetation NPP at each level so that we can evaluate the stability of vegetation NPP.

We divided the factors into static and dynamic factors. Static factors include geographical location, altitude, and slope, while dynamic factors include climate factors, water reserves, and human influence. Although this classification is more comprehensive than previous analysis, it can be seen from this study that the two types of factors are closely related. Factors like accumulated temperature and sunshine duration might be influenced by elevation, which can further affect NPP. A more detailed examination of the interactions between factors is essential for comprehensive analysis. Some existing studies have shown a significant correlation between changes in water yield and changes in NPP, but in those studies, water yield is the difference between precipitation and evapotranspiration, which may introduce some errors in water quantity estimation [58,62,63,71]. It may be more appropriate to use TWS as the water factor, which can affect NPP [67]. This study introduced TWS as a factor affecting vegetation NPP in the YRB. While it has been identified as important, there is still a need for further research to understand the complex processes involved in how TWS is consumed by vegetation and the implications for hydrology and ecology.

**Data Variety and Completeness:** The dataset used in this study comprises a variety of factors with differing time spans. The NPP data covers the years 2000–2022, but climate data (such as accumulated temperature, sunshine duration, precipitation, and temperature) is available only from 2000 to 2019. It should be noted that the water reserve data is monthly, and in order to adjust to annual data, this article adopts the average method. Due to the discontinuity of water storage data, although some scholars have proposed using interpolation methods to fill in, this article has selected years as neatly as possible (2003–2010, 2013, and 2016–2019) and averaged the total months of these 13 years (January, May, July, November, and December) as annual water storage data. The correlation analysis period is for these 13 years. This mismatch in data availability introduces potential errors, and using monthly water storage data to create annual averages could impact the accuracy of the results. When conducting single factor analysis, due to the fact that population density data is from a five-year period (2000, 2005, 2010, 2015, 2020), in order to unify the analysis, the four climate data (accumulated temperature, sunshine, precipitation, and temperature), water storage data, GDP data, and land use data for 2020 were all replaced by 2019. Therefore, there may also be single-factor analysis errors caused by incomplete data.

In conclusion, this study provides valuable insights into the factors influencing vegetation NPP in the YRB. However, future research should focus on addressing the discussed issues for a more accurate and comprehensive analysis.

## 5. Conclusions

In the study of spatiotemporal variation of vegetation NPP in the YRB, the spatial distribution of vegetation NPP in the YRB is highly uneven and exhibits significant differences. The NPP is smaller in the northwestern regions and becomes larger as one moves towards the southeastern areas. From 2000 to 2022, the YRB has shown an increasing trend in vegetation NPP, with the most significant changes occurring in the middle reaches of the basin. These changes are related to recent environmental protection policies, such as the establishment of ecological conservation zones and reforestation efforts.

In the analysis of the factors affecting vegetation NPP in the YRB, we find that different geographic locations, topography, and climate conditions have led to variations in vegetation NPP. In general, the southern parts of the YRB have higher NPP than the northern

ones; the eastern areas have higher NPP than the western ones. Compared with the trend of vegetation NPP in the YRB, there is a positive correlation with accumulated temperature, precipitation, and temperature, while a negative correlation exists with sunshine duration and TWS. In comparing contribution rates, we found that soil type, precipitation, and temperature had the most substantial influence on vegetation NPP in the region.

We particularly found that TWS shows a negative correlation with vegetation NPP in about 67% of the regions, which is nearly twice the area of positive correlation. This is primarily concentrated in the middle and lower reaches of the YRB, the region where vegetation NPP is increasing most rapidly. The reason for this negative correlation could be that vegetation growth consumes a significant amount of TWS. Correlation statistics indicate a strong relationship between changes in vegetation NPP and changes in TWS, making it necessary to explore the impact of TWS on vegetation NPP.

**Author Contributions:** K.T. designed the research; X.L., B.Z. and Z.W. researched and analyzed the data; G.X., K.C., P.X. and B.H. wrote the paper. All authors have read and agreed to the published version of the manuscript.

**Funding:** This work was supported by the National Natural Science Foundation of China (NSFC, 41974007, 42274003); Key Scientific and Technological Research Project of Henan Province (Grant No. 232102320280); the Key Laboratory of Geospace Environment and Geodesy, Ministry of Education, Wuhan University (21-01-05); Natural Science Foundation of Shandong Youth Foud (ZR2022QD144), Shandong Provincial Department of Science and Technology; Doctoral Research Initiation Fund of Shandong University of Technology (05827); Hubei University of Science and Technology 2023 First Batch of Doctoral Research Initiation Project (Si Xiong); Scientific Innovation Project for Young Scientists in Shandong Provincial Universities (2022KJ224).

**Data Availability Statement:** This can be seen in Table 1.

**Conflicts of Interest:** The authors declare no conflicts of interest.

## References

- Misra, R. Primary productivity of the biosphere. *Agro-Ecosystems* **1979**, *5*. [[CrossRef](#)]
- Guo, B.; Yang, F.; Fan, Y.W.; Zang, W.Q. The dominant driving factors of rocky desertification and their variations in typical mountainous karst areas of Southwest China in the context of global change. *Catena* **2023**, *220*, 106674. [[CrossRef](#)]
- Bao, G.; Bao, Y.; Qin, Z.; Xin, X.; Bao, Y.; Bayarsaikan, S.; Zhou, Y.; Chuntai, B. Modeling net primary productivity of terrestrial ecosystems in the semi-arid climate of the Mongolian Plateau using LSWI-based CASA ecosystem model. *Int. J. Appl. Earth Obs. Geoinf.* **2016**, *46*, 84–93. [[CrossRef](#)]
- Zhang, Y.; Wang, Q.; Wang, Z.; Yang, Y.; Li, J. Impact of human activities and climate change on the grassland dynamics under different regime policies in the Mongolian Plateau. *Sci. Total Environ.* **2020**, *698*, 134304. [[CrossRef](#)] [[PubMed](#)]
- Ruimy, A.; Saugie, B.; Dedieu, G. Methodology for the estimation of terrestrial net primary production from remotely sensed data. *J. Geophys. Res.* **1994**, *99*, 5263–5283. [[CrossRef](#)]
- Field, C.B.; Behrenfeld, M.J.; Randerson, J.T.; Falkowski, P. Primary production of the biosphere: integrating terrestrial and oceanic components. *Science* **1998**, *281*, 237–240. [[CrossRef](#)] [[PubMed](#)]
- Cao, H.J. Estimation and Spatiotemporal Evolution of Net Primary Productivity of Vegetation in the Hexi Corridor Based on Random Forests. Master's Thesis, Northwest Normal University, Lanzhou, China, 2019.
- Anderson, R.G.; Goulden, M.L. Relationships between climate, vegetation, and energy exchange across a montane gradient. *J. Geophys. Res.* **2011**, *116*, G01026. [[CrossRef](#)]
- Du, W. Temporal and Spatial Changes of Forest Biomass in China and Its Response to Climate Change. Master's Thesis, Nanjing Forestry University, Nanjing, China, 2018.
- Jin, K. Spatial and Temporal Changes in Vegetation Cover in China and Their Relationship with Climate and Human Activities. Ph.D. Thesis, Northwest A&F University, Xianyang, China, 2019.
- Fang, J.; Piao, S.; Field, C.B.; Pan, Y.; Guo, Q.; Zhou, L.; Peng, C.; Tao, S. Increasing net primary production in China from 1982 to 1999. *Ecol. Soc. Am.* **2003**, *1*, 293–297. [[CrossRef](#)]
- Gang, C.; Zhao, W.; Zhao, T.; Zhang, Y.; Gao, X.; Wen, Z. The impacts of land conversion and management measures on the grassland net primary productivity over the Loess Plateau, Northern China. *Sci. Total Environ.* **2018**, *645*, 827–836. [[CrossRef](#)]
- Yuan, Z.H.; Lei, J.; Bao, G.; Sa, C.L.; Suri, G.G.; Chi, Y.F. The impact of land use/cover change on vegetation coverage in the Hunshandak sandy land. *J. Soil Water Conserv.* **2016**, *30*, 330–338.
- Sun, Y.; Yang, Y.; Zhang, Y.; Wang, Z. Assessing vegetation dynamics and their relationships with climatic variability in northern China. *Phys. Chem. Earth* **2015**, *87–88*, 79–86. [[CrossRef](#)]

15. Dong, S.Y.; Liu, W.W. Implementing the New Development Concept to Assist in Carbon Peak and Carbon Neutrality. *People's Daily*, 11 April 2023.
16. De Marco, A.; Fioretto, A.; Giordano, M.; Innangi, M.; Menta, C.; Papa, S.; Virzo De Santo, A.C. Stocks in Forest Floor and Mineral Soil of Two Mediterranean Beech Forests. *Forests* **2016**, *7*, 181. [[CrossRef](#)]
17. Hazarika, M.K.; Yasuoka, Y.; Ito, A.; Dye, D. Estimation of net primary productivity by integrating remote sensing data with an ecosystem model. *Remote Sens. Environ.* **2005**, *94*, 298–310. [[CrossRef](#)]
18. Zhou, Y.; Xing, B.; Ju, W. Assessing the impact of urban sprawl on net primary productivity of terrestrial ecosystems using a process-based model—A case study in Nanjing, China. *IEEE J. Sel. Top. Appl. Earth Obs. Remote Sens.* **2015**, *8*, 2318–2331. [[CrossRef](#)]
19. Zhang, R.; Zhou, Y.; Luo, H.; Wang, F.; Wang, S. Estimation and analysis of spatiotemporal dynamics of the net primary productivity integrating efficiency model with process model in karst area. *Remote Sens.* **2017**, *9*, 477. [[CrossRef](#)]
20. Zhou, W.; Mou, F.Y.; Gang, C.C.; Guan, D.J.; He, J.F.; Li, J.L. The spatiotemporal dynamics of net primary productivity of grasslands in China from 1982 to 2010 and its relationship with climate factors. *J. Ecol.* **2017**, *37*, 4335–4345.
21. Yang, X.; Guo, B.; Han, B.M.; Chen, S.T.; Yang, F.; Fan, Y.W.; He, T.L.; Liu, Y. Analysis of the spatiotemporal evolution pattern and driving mechanism of NPP in the Qinghai Tibet Plateau. *Resour. Environ. Yangtze River Basin* **2019**, *28*, 3038–3050.
22. Lu, L.; Li, X.; Frank, V. Remote sensing estimation of net primary productivity of vegetation in the Heihe River Basin. *J. Desert Res.* **2005**, *6*, 31–38.
23. Lieth, H. Primary production: Terrestrial ecosystems. *Hum. Ecol.* **1973**, *1*, 303–332. [[CrossRef](#)]
24. Running, S.W.; Hunt, E. Generalization of a Forest Ecosystem Process Model for Other Biomes, BIOME-BGC, and an Application for Global-Scale Models. In *Scaling Physiological Processes*; Academic Press, Inc.: San Diego, CA, USA, 1993; pp. 141–158.
25. Potter, C.S.; Randerson, J.T.; Field, C.B.; Matson, P.A.; Vitousek, P.M.; Mooney, H.A.; Klooster, S.A. Terrestrial ecosystem production: A process model based on global satellite and surface data. *Glob. Biogeochem. Cycles* **1993**, *7*, 811–841. [[CrossRef](#)]
26. Field, C.B.; Randerson, J.T.; Malmstrom, C.M. Global net primary production: Combining ecology and remote sensing. *Remote Sens. Environ.* **1995**, *51*, 74–88. [[CrossRef](#)]
27. Zhou, G.S.; Zhang, X.S. A Preliminary Study on the Net Primary Productivity Model of Natural Vegetation. *J. Plant Ecol.* **1995**, *19*, 193–200.
28. Xiao, F.J.; Liu, Q.F.; Xu, Y.Q. Estimation of Terrestrial Net Primary Productivity in the Yellow River Basin of China Using Light Use Efficiency Model. *Sustainability* **2022**, *14*, 7399. [[CrossRef](#)]
29. Mowll, W.; Blumenthal, D.M.; Cherwin, K.; Symstad, A.J.; Vermeire, L.T.; Collins, S.L.; Smith, M.D.; Knapp, A.K. Climatic controls of aboveground net primary production in semi-arid grasslands along a latitudinal gradient portend low sensitivity to warming. *Oecologia* **2015**, *177*, 959–969. [[CrossRef](#)] [[PubMed](#)]
30. Terwayet, B.O.; Zhang, W.C.; Terwayet, B.H. Assessment of drought characteristics and its impacts on net primary productivity (NPP) in southeastern Tunisia. *Arab. J. Geosci.* **2022**, *16*, 26. [[CrossRef](#)]
31. Seino, H.; Uchijima, Z. Agroclimatic Evaluation of Net Primary Productivity of Natural Vegetation: Assessment of Total Net Primary Production in Japan. *J. Agric. Meteorol.* **1985**, *41*, 139–144. [[CrossRef](#)]
32. Vernet, M.; Ellingsen, I.; Marchese, C.; Bélanger, S.; Cape, M.; Slagstad, D.; Matrai, P.A. Spatial variability in rates of Net Primary Production (NPP) and onset of the spring bloom in Greenland shelf waters. *Prog. Oceanogr.* **2021**, *198*, 102655. [[CrossRef](#)]
33. Li, D.K.; Wang, Z. Analysis of NPP Change Characteristics of Land Vegetation in China Based on MOD17A3. *J. Ecol. Environ.* **2018**, *27*, 397–405.
34. Hong, C.Q. Research on the Impact of NPP Based Land Remediation on Cultivated Land Productivity. Master's Thesis, Nanjing University of Information Technology, Nanjing, China, 2018.
35. Li, L. Research on the Impact of Climate Change and Human Activities on NPP Changes of Vegetation in Northwest China. Master's Thesis, Shaanxi Normal University, Xi'an, China, 2019.
36. Zhang, Y.Z.; Gong, J.; Yang, J.X.; Peng, J. Evaluation of Future Trends Based on the Characteristics of Net Primary Production (NPP) Changes over 21 Years in the Yangtze River Basin in China. *Sustainability* **2023**, *15*, 10606. [[CrossRef](#)]
37. Lagomarsino, A.; Mazza, G.; Agnelli, A.E.; Lorenzetti, R.; Bartoli, C.; Viti, C.; Colombo, C.; Pastorelli, R. Litter fractions and dynamics in a degraded pine forest after thinning treatments. *Eur. J. For. Res.* **2020**, *139*, 295–310. [[CrossRef](#)]
38. Li, Y.L.; Pan, X.Z.; Wang, C.K.; Liu, Y.; Zhao, Q.G. The spatiotemporal distribution characteristics and driving factors of net primary productivity of vegetation in Guangxi from 2000 to 2011. *J. Ecol.* **2014**, *34*, 5220–5228.
39. Zhang, F.; Zhou, G.S.; Wang, Y.H. Dynamic simulation of net primary productivity of typical grassland vegetation in Inner Mongolia based on CASA model. *J. Plant Ecol.* **2008**, *4*, 786–797.
40. Piao, S.L.; Fang, J.Y.; He, J.S. Variations in vegetation net primary production in the Qinghai-Xizang plateau, China, from 1982 to 1999. *Clim. Chang.* **2006**, *74*, 253–267. [[CrossRef](#)]
41. Zhang, K.; Zhu, C.M.; Ma, X.D.; Zhang, X.; Yang, D.H.; Shao, Y.K. Spatiotemporal Variation Characteristics and Dynamic Persistence Analysis of Carbon Sources/Sinks in the Yellow River Basin. *Remote Sens.* **2023**, *15*, 323. [[CrossRef](#)]
42. Jiang, T.; Wang, X.L.; Afzal, M.M.; Sun, L.; Luo, Y. Vegetation Productivity and Precipitation Use Efficiency across the Yellow River Basin: Spatial Patterns and Controls. *Remote Sens.* **2022**, *14*, 5074. [[CrossRef](#)]
43. Yang, Y.J.; Li, H.Y. Monitoring spatiotemporal characteristics of land-use carbon emissions and their driving mechanisms in the Yellow River Delta: A grid-scale analysis. *Environ. Res.* **2022**, *214*, 114151. [[CrossRef](#)]

44. Zhang, Z.W.; Liu, Y.F. Spatial Expansion and Correlation of Urban Agglomeration in the Yellow River Basin Based on Multi-Source Nighttime Light Data. *Sustainability* **2022**, *14*, 9359. [[CrossRef](#)]
45. Liu, S.C.; Shao, Q.Q.; Ning, J.; Niu, L.N.; Zhang, X.Y.; Liu, G.B.; Huang, H.B. Remote-Sensing-Based Assessment of the Ecological Restoration Degree and Restoration Potential of Ecosystems in the Upper Yellow River over the Past 20 Years. *Remote Sens.* **2022**, *14*, 3550. [[CrossRef](#)]
46. Tian, H.W.; Ji, X.J.; Zhang, F.M. Spatiotemporal variations of vegetation net primary productivity and its response to meteorological factors across the yellow river basin during the period 1981–2020. *Front. Environ. Sci.* **2022**, *10*, 949564. [[CrossRef](#)]
47. Zhang, F.; Hu, X.S.; Zhang, J.; Li, C.Y.; Zhang, Y.P.; Li, X.L. Change in Alpine Grassland NPP in Response to Climate Variation and Human Activities in the Yellow River Source Zone from 2000 to 2020. *Sustainability* **2022**, *14*, 8790. [[CrossRef](#)]
48. Xue, S.B.; Ma, B.; Wang, C.G.; Li, Z.B. Identifying key landscape pattern indices influencing the NPP: A case study of the upper and middle reaches of the Yellow River. *Ecol. Model.* **2023**, *484*, 110457. [[CrossRef](#)]
49. Wei, Z.Y.; Jian, Z.; Sun, Y.J.; Pan, F.; Han, H.F.; Liu, Q.H.; Mei, Y. Ecological sustainability and high-quality development of the Yellow River Delta in China based on the improved ecological footprint model. *Sci. Rep.* **2023**, *13*, 3821. [[CrossRef](#)] [[PubMed](#)]
50. Song, Y.; Liang, T.; Zhang, L.B.; Hao, C.Z.; Wang, H. Spatio-Temporal Changes and Contribution of Human and Meteorological Factors to Grassland Net Primary Productivity in the Three-Rivers Headwater Region from 2000 to 2019. *Atmosphere* **2023**, *14*, 278. [[CrossRef](#)]
51. Xuan, W.X.; Rao, L.Y. Spatiotemporal dynamics of net primary productivity and its influencing factors in the middle reaches of the Yellow River from 2000 to 2020. *Front. Plant Sci.* **2023**, *14*, 1043807. [[CrossRef](#)] [[PubMed](#)]
52. Chen, S.; Zhang, Q.; Chen, Y.; Zhou, H.; Xiang, Y.; Liu, Z.; Hou, Y. Vegetation Change and Eco-Environmental Quality Evaluation in the Loess Plateau of China from 2000 to 2020. *Remote Sens.* **2023**, *15*, 424. [[CrossRef](#)]
53. Zhu, Z.Y.; Mei, Z.K.; Li, S.L.; Ren, G.X.; Feng, Y.Z. Evaluation of Ecological Carrying Capacity and Identification of Its Influencing Factors Based on Remote Sensing and Geographic Information System: A Case Study of the Yellow River Basin in Shaanxi. *Land* **2022**, *11*, 1080. [[CrossRef](#)]
54. Hong, L.L.; Shen, Y.; Ma, H.B.; Zhang, P.; Huo, X.-R.; Wen, H.-C. Temporal and spatial variation of vegetation net primary productivity and its driving factors in Ningxia, China from 2000 to 2019. *J. Appl. Ecol.* **2022**, *10*, 2769–2776.
55. Zhang, X.N.; Nian, L.L.; Liu, X.Y.; Samuel, A.; Yang, Y.B.; Li, X.D.; Wang, Q.X. The spatiotemporal response of photosynthetic accumulation per leaf area to climate change on alpine grassland. *Glob. Ecol. Conserv.* **2023**, *43*, e02467. [[CrossRef](#)]
56. Wang, Z.L.; Dong, C.; Dai, L.; Wang, R.Y.; Liang, Q.; He, L.H.; Wei, D. Spatiotemporal evolution and attribution analysis of grassland NPP in the Yellow River source region, China. *Ecol. Inform.* **2023**, *76*, 102135. [[CrossRef](#)]
57. Tian, Z.H.; Qin, T.L.; Wang, H.L.; Li, Y.Z.; Yan, S.; Hou, J.; Abebe, S.A. Delayed response of net primary productivity with climate change in the Yiluo River basin. *Front. Earth Sci.* **2023**, *10*, 1017819. [[CrossRef](#)]
58. Wei, H.J.; Xue, D.; Huang, J.C.; Liu, M.X.; Li, L. Identification of Coupling Relationship between Ecosystem Services and Urbanization for Supporting Ecological Management: A Case Study on Areas along the Yellow River of Henan Province. *Remote Sens.* **2022**, *14*, 2277. [[CrossRef](#)]
59. Wang, J.X.; Qiu, S.K.; Du, J.; Meng, S.W.; Wang, C.; Teng, F.; Liu, Y.Y. Spatial and Temporal Changes of Urban Built-Up Area in the Yellow River Basin from Nighttime Light Data. *Land* **2022**, *11*, 1067. [[CrossRef](#)]
60. Guo, B.; Liu, Y.F.; Fan, J.F.; Lu, M.; Zang, W.; Liu, C.; Wang, B.; Huang, X.; Lai, J.; Wu, H. The salinization process and its response to the combined processes of climate change–human activity in the Yellow River Delta between 1984 and 2022. *Catena* **2023**, *231*, 107301. [[CrossRef](#)]
61. Zhang, X.N.; Nian, L.L.; Liu, X.Y.; Li, X.D.; Adingo, S.; Liu, X.L.; Zhang, Y.Q. Spatial–Temporal Correlations between Soil pH and NPP of Grassland Ecosystems in the Yellow River Source Area, China. *Int. J. Environ. Res. Public Health* **2022**, *19*, 8852. [[CrossRef](#)] [[PubMed](#)]
62. Zhou, J.; Zhang, B.; Zhang, Y.W.; Su, Y.; Chen, J.; Zhang, X. Research on the Trade-Offs and Synergies of Ecosystem Services and Their Impact Factors in the Taohe River Basin. *Sustainability* **2023**, *15*, 9689. [[CrossRef](#)]
63. Shao, Y.J.; Liu, Y.S.; Li, Y.H.; Yuan, X.F. Regional ecosystem services relationships and their potential driving factors in the Yellow River Basin, China. *J. Geogr. Sci.* **2023**, *33*, 863–884. [[CrossRef](#)]
64. Tian, K.J.; Wang, Z.T.; Li, F.P.; Gao, Y.; Xiao, Y.; Liu, C. Drought Events over the Amazon River Basin (1993–2019) as Detected by the Climate-Driven Total Water Storage Change. *Remote Sens.* **2021**, *13*, 1124. [[CrossRef](#)]
65. Wang, Z.T.; Tian, K.J.; Li, F.P.; Xiong, S.; Gao, Y.; Wang, L.; Zhang, B. Using Swarm to Detect Total Water Storage Changes in 26 Global Basins (Taking the Amazon Basin, Volga Basin and Zambezi Basin as Examples). *Remote Sens.* **2021**, *13*, 2659. [[CrossRef](#)]
66. Box, E.; Lieth, H.; Wolaver, T. Miami model productivity map. In primary production of terrestrial ecosystems. *Hum. Ecol.* **1982**, *1*, 303–332.
67. Chen, S.T.; Guo, B.; Yang, F.; Han, B.M.; Fan, Y.W.; Yang, X.; He, T.L.; Liu, Y.; Yang, X.W. The spatiotemporal variation pattern of vegetation NPP on the Qinghai Tibet Plateau from 2000 to 2015 and its response to climate change. *J. Nat. Resour.* **2020**, *35*, 2511–2527.
68. Thorpe, J.; Wolfe, S.A.; Houston, B. Potential impacts of climate change on grazing capacity of native grasslands in the Canadian prairies. *Can. J. Soil Sci.* **2008**, *88*, 595–609. [[CrossRef](#)]
69. Ju, L.J.; Ouyang, X.Z.; Pan, P.; Liu, J.; Zhou, Q.Q.; Ye, Q.L. The spatiotemporal changes of net primary productivity of forests in Gannan from 2000 to 2019 and their relationship with climate factors. *J. Northeast For. Univ.* **2022**, *50*, 37–44.

70. Wang, J.F.; Xu, C.D. Geographic detectors: Principles and prospects. *J. Geogr.* **2017**, *72*, 116–134.
71. Wang, G.; Yue, D.P.; Yu, Q. Regulated Ecosystem Services Trade-Offs: Synergy Research and Driver Identification in the Vegetation Restoration Area of the Middle Stream of the Yellow River. *Remote Sens.* **2022**, *14*, 718. [[CrossRef](#)]
72. Ma, D.L.; Huang, Q.J.; Liu, B.Z.; Zhang, Q. Analysis and Dynamic Evaluation of Eco-Environmental Quality in the Yellow River Delta from 2000 to 2020. *Sustainability* **2023**, *15*, 7835. [[CrossRef](#)]

**Disclaimer/Publisher’s Note:** The statements, opinions and data contained in all publications are solely those of the individual author(s) and contributor(s) and not of MDPI and/or the editor(s). MDPI and/or the editor(s) disclaim responsibility for any injury to people or property resulting from any ideas, methods, instructions or products referred to in the content.